Lab on a Chip

CRITICAL REVIEW

View Article Online
View Journal | View Issue

Cite this: *Lab Chip*, 2022, **22**, 3603

Flowmetering for microfluidics

C. Cavaniol, *[ab] W. Cesar,[b] S. Descroix [a] and J.-L. Viovy *[a]

Received 24th February 2022,
Accepted 29th May 2022

DOI: 10.1039/d2lc00188h

rsc.li/loc

Originally designed for chromatography, electrophoresis, and printing technologies, microfluidics has since found applications in a variety of domains such as engineering, chemistry, environmental, and life sciences. The fundamental reason for this expansion has been the development of miniature components, allowing the handling of liquids at the microscale. For the maturation of microfluidic technologies, the need for affordable, reliable, and quantitative techniques to measure flow rates from 1 nL min^{-1} to 1 mL min^{-1} appears as a strong challenge. We review herein the different technologies available and those under development, and discuss their sensing principles and industrial maturity. Given the need of traceability of these measurements, we then focus on the developments of primary standards to measure microfluidic flow rates by metrological institutes. We conclude this review with some perspectives and pending challenges for microfluidic flowmeters.

1 Introduction

The field of microfluidics emerged in the 70's, and has since grown in a quasi-exponential way, becoming one of the main empowering technologies in biology and medicine (see ref. 1–3 for reviews). Microfluidics was defined by Stone *et al.* as the "devices and methods for controlling and manipulating fluid flows with length scales less than a millimeter".[4] Practical achievements, however, had already been proposed earlier. In 1965, Richard Sweet at Standford University developed an inkjet printer using a vibrating nozzle with a 35 μm hole,[5] which is regarded as the first microfluidic device.[3,6] This work was continued by Bassous *et al.* at IBM.[7] Inkjet printing is now a multibillion US$ market, and is still based on microfluidics, making it, volume-wise, a major field of application. The next step in microfluidics history was initiated at Standford University by Terry *et al.*, who developed the first miniaturized gas chromatograph using a silicon wafer.[8,9] Microfluidics has since then raised interest in a constantly increasing range of applications, taking advantage of several unique features: i/in direct inspiration from microelectronics, microfluidics allows to achieve high integration, automation, and parallelization of multiple steps (leading to the concept of "microfluidic processor" and "Micro-Total Analysis System", a term first coined by Widmer and Manz[10]); ii/microfluidics allows the reliable manipulation of sub-microliter quantities of fluids, and thus a dramatic reduction in this device's sizes and the required sample and reagent quantities; iii/finally, microfluidics has also opened the route to intrinsically new concepts, such as "digital PCR"[11,12] or "organs on chip".[13–15] These intrinsic advantages have resonated with biological and medical markets, in which reagents and samples can be extremely limited and expensive, and the development of systems in biology and molecular medicine has called for massively parallel analyses. In 2013, the microfluidic market was valued at US$ 1.6 billion,[16] and is expected to reach US$ 44.0 billion by 2025.[17] This high growth rate is largely due to recent applications in genomics, point-of-care diagnostics, and drug delivery systems.[18–20] However, such an expansion could only be achieved thanks to the development of functional components, allowing the handling of liquids at the microscale and, in particular, in actuators and sensors.[21,22] According to the market survey *Results survey on microfluidics flow control* performed in 2015 with industrial and academic players in microfluidics by enabling MNT,[23] the properties of fluids used vary significantly depending on the application, from gas to liquid, aqueous to organic, monophasic or a multi phasic, Newtonian or not, with a viscosity ranging from 1 to 1000 mPa s. Moreover, flow conditions may also vary widely with commonly applied flow rates ranging from 1 nL min^{-1} to 1 mL min^{-1} in continuous or pulsating mode. Lastly, temperature and pressure ranges can vary from 0 to 100 °C and from 0 to 30 bar, respectively. Considering these disparities, an ideal flowmeter must be able to measure the flow rate over a very wide range and independent of the nature of the liquid, irrespective of the ambient conditions. Covering all these conditions with a single device is probably an unattainable challenge, while providing the community with a set of technologies suitable for different ranges of applications would certainly be an acceptable situation. As measurement tools, these flowmeters belong to the large field of metrology, the scientific domain related to measurement. To compare and

[a] *Institut Curie and Institut Pierre Gilles de Gennes, PSL Research University, CNRS UMR 168, Paris, France. E-mail: charles.cavaniol@curie.fr*
[b] *Fluigent SAS, Kremlin-Bicêtre, France*

discuss the accuracy and reliability of different flowmeters, it appears fundamental to be able to trace these measurements to a common reference material. The International Vocabulary of Metrology (VIM) defines the traceability as "the property of a measurement result whereby the result can be related to a reference through a documented unbroken chain of calibrations, each contributing to the measurement uncertainty".[24] A reference can be considered as a measurement unit through its practical realization, or a measurement procedure including the measurement unit for a non-ordinal quantity, or a measurement standard. Such standards, called as primary standards, are provided by metrological institutes to allow measurement traceability to the International System of Units. Herein, we review the current technologies and devices dedicated to flow measurement in microfluidics. To do so, we will first describe the main operating principles of the existing flow measurement methods, focusing on their strengths and weaknesses, and discuss their respective level of maturity. To cover a large number of applications, herein, we have focused on sensors capable of measuring Newtonian's liquid flow rates ranging from 1 nL min^{-1} to 1 mL min^{-1}. Indeed, except the early state-of-the-art done by Gravesen *et al.*, the other reviews in the field are fully or partially dedicated to microfluidic flowmeters for gases.[22] Given the importance of microfabrication techniques in the development of microfluidics, since the 90s, most reviews have focused on MEMS-based flowmeters[21,22,25–27] and classified them according to their working principle based on the theoretical framework, *e.g.*, thermal and non-thermal. These works also depict the fabrication process including the materials used, their transducing principle, and performances. More recently, different approaches to review microfluidic flowmeters have been found, either focusing on cantilever-based flowmeters[28,29] or on flowmeters for biomedical applications.[30] In comparison with other reviews, herein, we also propose to the reader a new perspective on the field by discussing the recent developments of primary standards for microfluidic flows by metrological institutes.

2 Flow rate measurements at the microscale

First manufactured using MEMS techniques, flow sensors have accompanied and enabled the development of microfluidics. The need for liquid flows measurements of small value initially arose with the development of liquid chromatography. In 1974, Van Putten *et al.* manufactured a miniature sensor able to measure microfluidic gas flows based on a technique called hot-wire anemometry (HWA).[31] The first liquid flow sensor for microfluidics, based on a time-of-flight (TOF) technology, was developed by Miller *et al.* in 1982.[32] In the 1990s, the rapid growth of microfluidics led to a diversification of flow rate measurement methods. Some of these technologies reached the industrialization stage and are now available in the market. With the benefits of PDMS-based microdevices and the emergence of new applications, other methods have been developed but remain at the proof-of-concept stage to date. To describe the different flow sensors technologies, we divided the measuring principles into two categories active and passive sensors (Fig. 1):

- We define an active sensor as a system that supplies energy to the liquid to measure its disturbance. Active sensors are divided into thermal and Coriolis flowmeters. Thermal sensors heat the liquid and measure the heat transport to obtain the flow rate. In Coriolis sensors, the channel through which the liquid flows is excited to generate a force called the Coriolis force. This force results in a second motion of the channel whose amplitude is used to measure the flow rate. Together, both technologies represent more than two-thirds of the flow sensors used in microfluidics.[33]
- We define a passive sensor as a system that does not supply any energy to disturb the fluid. Here, the liquid dissipates energy in the sensor body. We identify them according to their transducing principle. First, the flow rate is determined through the measurement of the sensor body movement or deformation (fluid–structure interaction). Second, the traditional gravimetric method measures the mass of the flowing liquid over time, while more recently, the advance of the meniscus front tracked in a capillary at the exit of the microfluidic circuit has been used to measure the flow rate, similar to a macroscopic bubble flowmeter. The last two principles will be further discussed in the section related to the development of primary standards by metrological institutes.

2.1 Active flowmeters

2.1.1 Thermal flowmeters. Thermal flowmeters are the most commonly used sensors to measure microfluidic flows.[22,25–27] They are based on heat transfer measurement. In general, thermal flow sensors consist of two parts: a heating element and a sensing element, which detect the

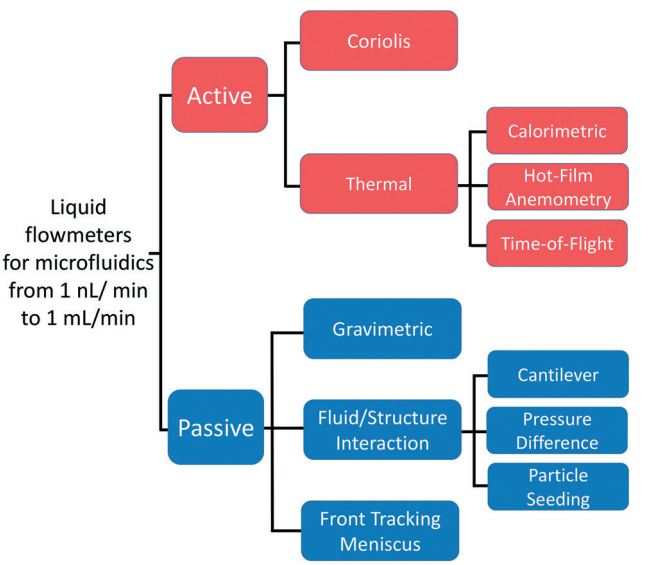

Fig. 1 Mapping of the different flow rate measurement principles for microfluidics.

variation in heat transfer between the heater and the surrounding flow. Here, the sensor sensitivity increases with the heat transferred to the working fluid. Three different measurement principles have been reported in the literature, as shown in Fig. 2.

First, the hot-wire and hot-film anemometry (HFA) measure the heat transfer from a hot body to the flowing fluid (Fig. 2A). The heating element is also used as a heat dissipation sensor. With HWA, a resistive wire sensor is set within the fluid flow, whereas for HFA, a thin film resistive sensor is placed adjacent to the flow. According to King's law,[34] the heat loss Q_h can be related to the fluid velocity v as

$$Q_h = a + b\sqrt{v} \quad (1)$$

where a and b are constants that depend on the channel geometry, temperature, materials used, and, more importantly, on the fluid thermal properties. These constants have to be determined empirically.[22] The heat loss results from the temperature difference between the liquid and the hot body. Using HWA, the temperature of the wire can be obtained through its resistance measurement

$$R(T) = R(T_0)[1 + \alpha(T - T_0)] \quad (2)$$

where $R(T)$ is the electrical resistance at temperature T and α is the temperature coefficient of resistivity.[26] Because the dissipated heat is proportional to the dissipated power:

$$Q \propto P = R(T)I^2$$

where I is the current intensity. Anemometer sensors either operate in constant temperature mode or in constant current mode. The constant temperature mode requires a feedback circuitry that monitors and holds the sensor temperature constant. Thus, the power required increases with the fluid flow rate. In the constant current mode, as the flow rate increases, the heater temperature decreases. This temperature change is obtained through resistance or voltage measurements.[25] HWA sensors are generally distant from the substrate, which enables optimal heating uniformity and high sensitivity, but they are more fragile than HFA sensors.[27] Moreover, the thin film resistor can be embedded within the microchannel wall, as shown by Wu *et al.*[35] Although this may reduce its sensitivity, it allows for a much longer lifetime. Thus, hot-film technology better suits microfluidic flow rate measurements. From investigations on the materials used, the authors measured flow rates down to tens of nL min^{-1} and also highlighted the possibility to measure fluid changes such as bubbles. Since air has a lower heat capacity and thermal conductivity than the liquid, the temperature sensor measures a sudden temperature rise. Low sensitivity and power consumption are the main limitations of this measurement method. In addition, the flow direction cannot be identified.

Another thermal principle measurement has been developed that partly overcomes the problems encountered by HWA sensors: the calorimetric principle (Fig. 2B). Here, two or more thermal sensors are placed around the heater.[25,36] Calorimetric sensors measure the temperature asymmetry caused by the passing fluid using a constant current applied to the heater.[37] They consume less power than HWA sensors, and the two sensors on both sides of the heater allow to determine the flow direction. However, calorimetric sensors have two main limitations: non-linearity and sensitivity. The measurement saturates over a certain flow rate, which is assumed to be related to the limited heat transfer between the liquid and both the sensor and heater filament surfaces.[38,39] For instance, Dijkstra *et al.* were able to measure water flow rates down to 40 nL min^{-1}, but the sensor was saturated over 400 nL min^{-1}.[40] Generally, only a flow rate range over one order of magnitude could be measured.[27] Secondly, to increase the calorimetric sensor sensitivity, it is necessary either to bring the temperature sensors closer to the heater, which can increase the manufacturing cost, or to increase the temperature range, which can be problematic when flowing thermosensitive liquids (such as biological samples). Increasing the heater temperature can also lead to strong changes in the liquid density and viscosity.[41] For instance, Dijkstra *et al.* used a temperature range larger than 40 °C.[40] As a third alternative to increase the sensitivity, the channel diameter can also be reduced, which increases the liquid velocity and thus the heat convection. However, the risk of clogging also increases. Finally, the less commonly used technology is time-of-flight sensors (see Fig. 2C).[42] With TOF, a heat pulse is emitted from the heater and measured downstream by a temperature

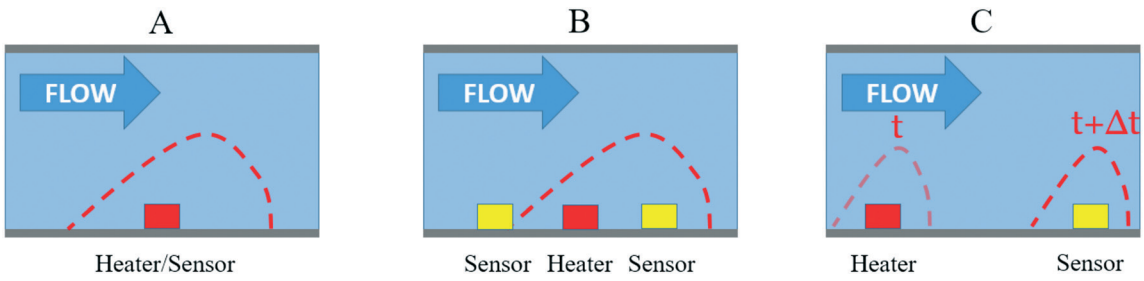

Fig. 2 Representation of different thermal flow principles: in A-hot wire anemometry, B-calorimetric, and C-time-of-flight. Red squares represent the heater element, while yellow squares show the sensor element. The red dashed lines represent the temperature distribution.

sensor. At least one heater and one thermal sensor are required to measure the flow rates. The same sensitivity problems as that in calorimetric sensors are encountered. In addition, the temperature diffusion along the channel is a major limitation of the TOF sensors. Indeed, the diffusion smoothes its temperature profile as a heat pulse is driven by the liquid, thus decreasing the measurement precision. However, Berthet *et al.* were able to reduce the signal-to-noise ratio using pseudostochastic temperature pulses and a cross correlation method between the detected and the injected signals.[43] They were also able to reduce the impact of the diffusion with several downstream sensors to obtain a linear flow rate measurement over two orders of magnitude with only a few degree Celsius operating range.

MEMS thermal flow sensors are usually regarded as the most mature flow sensor technology.[27] Since the 70s, MEMS technology has offered the ability to develop low-cost, scalable, and small device footprint thermal flow sensors with high sensitivity. Despite many drawbacks, the calorimetric principle is usually the sensing method used in commercially available flowmeters for microfluidic applications. The measurement depends strongly on the thermal properties of the liquid (thermal conductivity and diffusivity), thus requiring a calibration step for each liquid. Moreover, the measuring range of a sensor varies according to the liquid thermal properties. For instance, the M-flow unit sensor commercialized by Fluigent can measure flow rates from 1 to 80 μL min^{-1} when flowing water, but 20 to 500 μL min^{-1} for other liquids.[44] In addition, the measurement saturation drastically limits the sensor's dynamic range. Finally, to reduce the temperature differences used, the temperature sensors can be set closer to the heater. However, this complicates the manufacturing protocol, and therefore increases the sensor cost. To maintain a competitive price, the manufacturers have reduced the internal diameter of the channel to increase the sensitivity. As the measurement saturates, for each flow rate range, there is a corresponding internal diameter. For the lowest flow rates, the sensor diameter can be a limitation. Indeed, for water flows in the μL min^{-1} range or less, commercial sensors are 25 μm in diameter. Because their hydrodynamic resistance increases, their integration in a fluidic circuit may be compromised. Practically, they can be clogged very easily. Other thermal sensors can be found in the literature based on surface plasmon resonance temperature imaging, which is used to measure the heat dissipation similar to HFA sensors,[45] or thermal lens microscopy, which is used to generate a heat pulse similar to TOF sensors.[46] However, these principles will not be introduced in depth in this review as they do not represent credible technologies to measure microfluidic flow rates due to their very low maturity (only one scientific publication each), size, and complexity.

2.1.2 Coriolis flowmeters. The Coriolis flowmeter is a very promising technology to measure microfluidic flow rates as it overcomes several limitations induced by thermal flow sensors. The flow sensing is based on the Coriolis force applied to liquid movement. In 1835, Gustave-Gaspard Coriolis demonstrated that when a body moves in a rotating reference frame with respect to a Galilean frame of reference, it is subjected to an "inertial force" perpendicular to the movement direction.[47] In 1997, the first miniature Coriolis flowmeter was developed by Enoksson *et al.* to measure gas and water flows using MEMS fabrication processes.[48] The contribution of these manufacturing technologies allowed the sensor to quickly reach the industrial stage, and is currently commercialized by the Bronkhorst company as mini CORI-FLOW™.[49]

As shown in Fig. 3, the operation principle of the Coriolis flowmeter is based on the periodic rotation of the U-shape channel with an angular velocity ω_{act}.[50] This vibration is allowed due to the deposition of a conducting layer on top of the channel. By running an alternating current in the conductor while subjecting it to a constant magnetic field B, a periodical Lorentz force F_L is applied to the channel, which allows an oscillatory motion. As the mass flow Φ_m flows through the channel, the vibrations induce a perpendicular Coriolis force F_c. This force is proportional to the mass flow Φ_m and the angular velocity ω_{act}.

$$F_c = -2L_x(\omega_{act} \wedge \Phi_m) \quad (3)$$

The resulting Coriolis force induces an out-of-plane swinging vibration mode orthogonal to the actuation mode. More precisely, the channel has two swinging oscillation modes. The first mode, referred to as the actuation mode, is generated by the Lorentz force with an amplitude of oscillation Θ_{act}. The second, referred to as the detection mode, is induced by the Coriolis force with an amplitude of oscillation Θ_d. The flow rate can be extracted through the measurement of both amplitudes. Haneveld *et al.* showed that the two modes of the Coriolis mass flow sensor can be modelled as a second order system.[51] When the actuation

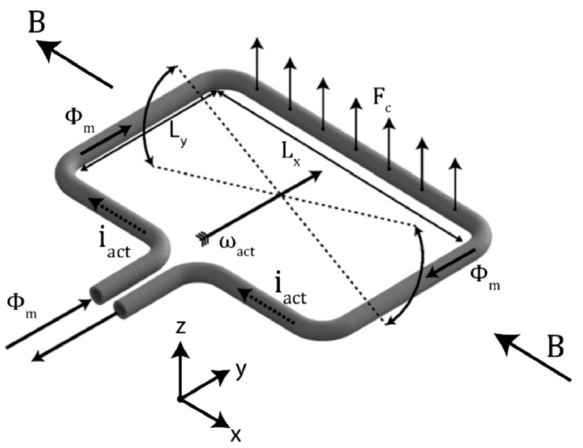

Fig. 3 Representation of the Coriolis flowmeter principle: the channel rotates periodically around the y axis with an angular velocity ω_{act}. When a mass flow Φ_m flows through the channel, a Coriolis force F_c will cause a secondary vertical motion.[118]

mode resonates at a frequency of $\omega_{act,r}$, the mass flow Φ_m can be measured as follows.

$$\Phi_m = \frac{AK_d\omega_{act,r}}{L_xL_y}\frac{\Theta_d}{\Theta_{act}} \quad (4)$$

where A is a constant that depends on the operating modes, K_d is the detection-mode modal spring constant, and L_x and L_y are the lengths of the microchannel, as defined in Fig. 3. However, the volume flow rate Q is usually required in microfluidics instead of mass flow rate Φ_m. Thus, it is necessary to measure the liquid density ρ as $\Phi_m = \rho Q$. However, the density can be measured using the resonant frequency $\omega_{act,r}$.[52]

$$\rho = \frac{K_d - 2\pi m_0\omega_{act,r}}{V2\pi m_0\omega_{act,r}} \quad (5)$$

where m_0 is the mass of the empty channel and V is the inner volume of the channel. With the Coriolis flowmeter, it is possible to measure both the volume flow Q and the liquid density. In contrast to a calorimetric sensor, the measurement is linear with respect to the flow rate over at least 3 orders of magnitude and does not require any calibration step.[50] Although the measurement is dependent on the liquid density, which can modify the accessible range of measurement, most liquids used in microfluidics remain within 1–2 kg m^{-3}. Despite these interesting features, the Coriolis flowmeter has still some limitations. During its operation, the working temperature of the sensor has been observed to slightly increase by some degrees during the measurement.[50] Similar to thermal sensors, this temperature increase can be a limitation when flowing thermosensitive liquids. Moreover, the internal volume V of the microchannel is reduced to measure very low flow rates (tens of nL min^{-1}). Typically, the commercial mini-CORI-FLOW™ sold by Bronkhorst has an internal diameter of 55 μm.[49] However, such a small channel could easily get clogged, especially when using multi-phase solid/liquid flows (*e.g.*, liquid with cells and beads) or simply with dust. In addition, its cost can be another limitation, being typically an order of magnitude more expensive than other commercial thermal sensors (see Table 1). Therefore, it does not meet the needs of a disposable sensor. And last, to our knowledge, the interactions between the magnetic field and the flowing liquid have not been studied yet, which could limit its use in microfluidic applications using magnetosensitive materials.

The Coriolis flowmeter represents a very promising alternative to the thermal sensors usually used in microfluidic applications. It does not require any calibration step, allows flow rate measurements over 3 orders of magnitude, and also allows the measurement of the liquid density. Although its price and internal diameter remain limitations in its use, it seems feasible to find a compromise between resolution, price, flow rate range, and internal diameter.

2.2 Passive flowmeters

As explained previously, passive sensors are identified according to their transducing principle: fluid/structure interaction, gravimetric, and front tracking meniscus. In this section, we will focus on fluid/structure interaction sensors; the other two will be introduced in the section on the

Table 1 Main features of liquid flow sensors for microfluidics. The flow ranges and their relative uncertainties were measured with water

Flowmeter	Range (μL min^{-1})	Relative uncertainty (%)	Response time (s)	Estimated price (€)	Estimated compacity (cm^3)	Ref.
Active sensors						
Calorimetric[a]	0.07–1.5	10	0.04	100–1000	50	57
	1–80	5	0.04	100–1000	50	58
	40–1000	5	0.04	100–1000	50	58
HFA	3–167	5	0.01	100–1000	50	59
	0.02–0.16	20–2.5	0.02	100–1000	50	35
	0.04–0.3	NA	NA	100–1000	50	40
TOF	10–1000	6	0.012	100–1000	50	43
Coriolis[a]	0.84–3300	0.2	0.2	2000–4000	400	60
Passive sensors						
Cantilever	2–35	0.1	NA	1000–5000	50 000	61
	5–500	0.1	0.01	400–2000	400	62
Pressure difference	1.1–1100	10	0.1	250–1000	1000	54
	1.7–1700	NA	NA	400–1000	50	56
Particle seeding	0.001–54	2–5	1	>10 000	>100 000	63
FTM	5–100	2	300	4000–8000	50 000	64
Gravimetric	0.1–1000	0.6–0.1	2	>10 000	>100 000	65, 66
	17–1.6 10^5	6–0.15	3	>10 000	>100 000	65–67
	0.017–1000	4–0.05	2	>10 000	>100 000	65, 66
	0.05–10 000	0.6–0.15	20	>10 000	>100 000	65, 66
	17–3300	0.62–0.06	10	5000	>100 000	65, 66
	2–100	6–100	2.5	3000	5000	63, 68

[a] These data correspond to industrial sensors (prices can vary depending on the packaging, hardware, software, and purchase volume).

development of primary standards by metrological institutes. The sensors based on fluid/structure interaction can be divided in subcategories depending on their measurement principle: (i) pressure difference measurement, (ii) cantilever bending, and (iii) motion of seeded particles. All these methods use the dissipation of energy from the liquid into a test body to either induce its motion or its deformation.

2.2.1 Pressure difference flowmeters. The principle of flow measurement by pressure difference is based on the Hagen–Poiseuille's law:

$$\Delta p = R_h(\eta)Q \quad (6)$$

where Δp is the pressure difference applied in the channel of hydrodynamic resistance R_h. By measuring the pressure difference between the inlet and outlet of a microchannel of known dimensions, it is possible to obtain the flow rate measurement. However, this measurement principle requires knowing the liquid viscosity. As R_h can be predicted theoretically or obtained from a calibration step, the major challenge of this technology relies on the measurement of the pressure downstream and upstream of the channel. This pressure measurement is carried out with a deformable diaphragm using different transduction principles with either a piezoresistive material deposited on the diaphragm[53,54] or with capacitive readouts (Fig. 4).[55,56] In the first case, when the pressure increases, the diaphragm deforms, resulting in a variation of the piezoresistive resistance. The resistance variation can be obtained from either current or voltage measurements. In the second case, an electrode is placed on the membrane and another one is fixed on top. The membrane deformation causes the gap length between the electrodes to decrease, which induces a change in the electric capacitance.

Although much progress has been made to increase the flow rate measurement ranges (up to 3 orders of magnitude[54,56]), this technology remains, to our knowledge, a proof-of-concept. Its limitations seem to have so far prevented attempts for its industrialization and commercialization. Indeed, flow rate measurement is based on prior knowledge of the liquid viscosity. As viscosity is temperature-dependent, the optimization of the experimental conditions is highly recommended.[53] In addition, sensor contaminations can be major sources of error. First, it can change the geometry of the channel, resulting in a hydrodynamic resistance variation. As shown by Oosterbroek *et al.*, a poor prediction of the channel hydrodynamic resistance can lead to a 20% error in the flow rate measurement.[55] This problem can be transitory due to the presence of dust during the experiment, but it can also persist because of clogging. Second, the pressure sensors can be contaminated by fouling, affecting the mechanical properties of the membrane, which would in turn result in a measurement bias.

2.2.2 Cantilever-based flowmeters. Drag force-based flowmeters have been developed to measure the flow rate for more than 25 years.[62] These sensors operate through the deflection of a cantilever in response to flow disturbances, as shown in Fig. 5(top). The beam is immersed perpendicular to the flow, and bends under the action of the fluid. Indeed, the movement of the fluid exerts a force (torque) called the drag force, which can be obtained by integrating the stress (times momentum arm) $[\sigma] = -p[I] + [\sigma']$ on the surface of the beam, with pressure p and viscous stress $[\sigma']$. The drag force (torque) is proportional to the fluid viscosity and velocity, and depends on the geometry of the system. The displacement/deformation of the cantilever can be modeled by the Euler–Bernoulli equation.[69] Thus, the degree of bending also depends on the Young's modulus of the material used and on the geometry of the cantilever through its moment of inertia. At low Reynolds numbers, cantilever bending is highly dependent on its confinement.[70] Thus, cantilever-based flowmeters can be classified according to their degree of confinement, as shown in Fig. 5. In the first case, the cantilever has the same size as that of the section, being confined in two directions similar to a cat-door. Noeth *et al.* proposed this geometry with an optical detection method, which consists of a reflection mirror deposited on the beam

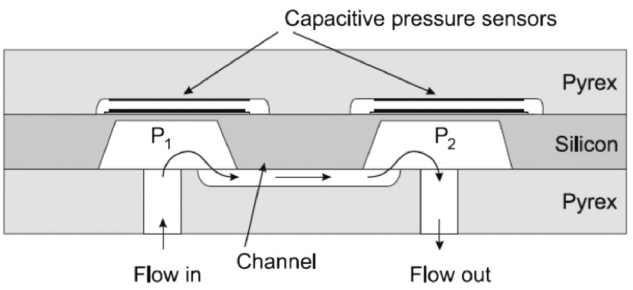

Fig. 4 Differential pressure flow rate sensor with capacitive readouts.[55]

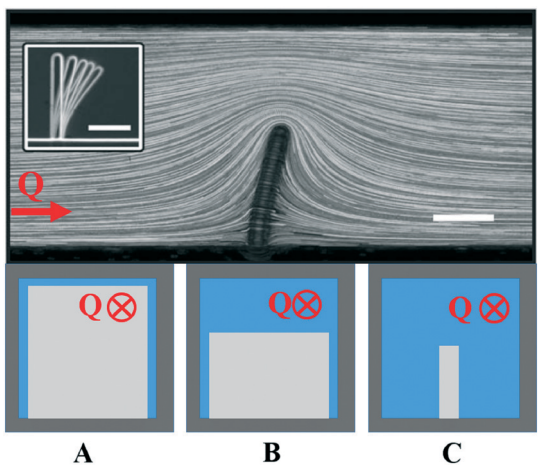

Fig. 5 On the top: Bending of a cantilever under flow with seeded particles, adapted from Wexler *et al.*[69] At the bottom: The different confinement degrees of the cantilever-based flowmeters: A-the cantilever is fully confined, B-the cantilever is only confined along one direction, C-the cantilever is not confined.

and a laser.[61,71] They were able to measure water flow rates from 2 to 35 μL min^{-1}. In order to limit the increase in the hydrodynamic resistance due to the obstruction of the channel by the beam, holes were added to the cantilever. By tuning the porosity, the authors were able to adapt the mechanical properties of the beam and thus vary the measuring ranges. However, as the holes clogged up, the mechanical properties varied, thus inducing a bias in the measurement.

In the second geometry, the beam is confined in one direction, leaving most of the fluid flowing at its tip. Proposed by Gass *et al.*, this configuration was used in the first cantilever-based flowmeter for microfluidics.[62] They were able to measure flow rates up to two orders of magnitude. As shown by Wexler *et al.*, this configuration allows the use of a depth-averaged model to predict the flow surrounding the cantilever.[69] In the regimes of small deflections and high confinement degrees, an analytical solution to the movement of the beam could be found. These authors showed analytically, experimentally, and by means of simulations that the beam follows two deformation regimes: below a certain flow rate the deformation is linear, then the deflection of the beam increases more slowly. However, these regimes will depend on the system parameters mentioned above such as the Young's modulus, degree of confinement, beam size, and the liquid's viscosity. As a variant of this strategy, Attia *et al.* proposed a system in which a drag-inducing element is immersed in the flow and retained by a spring-like deformable feature attached at the other side.[72] This approach is a direct transposition in microfluidics of the spring dynamometer. Stop-flow lithography[73,74] can be used to prepare springs with non-uniform properties, and thus extend the range of measurable flow rates. However, this approach raises problems of calibration, is difficult to model with quantitative theories, and shares with the previous one the disadvantage of mobile structures immersed in the liquid (risk of clogging or contamination, hydrodynamic resistance). Finally, the beam is neither confined in its length nor its height. In this geometry, the cantilever is located in the boundary layer thickness of the flow. Recently, great interest has been shown for this geometry of cantilever-based sensors as it mimicks hair-cells or cilia.[28,29,75,76] These mechanoreceptors are used by living systems as transducers for flow sensing and chemical sensing. Liu's group has been a pioneer in developing artificial hair-cell flow sensors, fabricated in either polymer or silicon material.[77,78] This sensor consists of an array of high aspect ratio cantilevers, each of them coupled to a strain gauge. The torque induced by the flow introduces a longitudinal strain that can be detected by the piezoresistors at the base. Using an array of cantilevers with different geometries, the authors were able to extend the range of measurable flow rates. It would also allow to adapt to the viscosity of the liquid. Among these 3 different configurations of cantilevers, it seems that this approach represents the most viable solution to meet the specifications of a flowmeter for microfluidics. Due to the low confinement of the beam, the hydrodynamic resistance of the sensor is only moderately increased. Moreover, the lesser the confinement of the beam, the lesser is the risk of clogging or deterioration. Finally, this configuration is more suitable toward a flowmeter, allowing to measure a wider range of flow rates for liquids of different viscosities.

Manufactured using MEMS techniques, cantilever-based flowmeters share some advantages with thermal flowmeters as they are compact and in the same price range. Contrary to thermal sensors, this technology can be adapted to liquids by manufacturing cantilever arrays. However, this technology has major shortcomings, which limit its transition to commercial use. As the deflection of the cantilever depends on the liquid's viscosity, a calibration step is necessary. Due to its transducing principle, the test body is set within the liquid flow so that it is exposed to contamination risks (liquid with seeded particles/cells, bubbles, or biochemical compounds such as proteins). The mechanical properties of a beam covered by chemical compounds would be affected, for *e.g.*, its thickness, overall elastic modulus, and moment of inertia, which will lead to a less deformable beam, and thus a measurement bias. Over a certain threshold force (torque) on the beam that could be exerted by either a pulse in the flow rate or by objects transported by the flow, bending can occur as plastic deformation, resulting in permanent bending. Worse, the cantilever could break, potentially reducing its lifetime.

2.2.3 Particle seeding. This principle of flow measurement is based on measuring the velocities of particles that have been seeded into the liquid. From the knowledge of the velocity profile, the flow rate within the channel can be obtained. Two main methods to measure the particle velocity have been developed: particle image velocimetry (PIV) and laser Doppler velocimetry (LDV). The principle of PIV is based on the correlation of two images of scattering particle ensembles. Two successive images of flow-tracing particles are recorded using a specified time delay. Typically, the two particle image fields are subdivided into uniformly spaced regions, known as interrogation areas, which are cross-correlated to determine the most probable local displacement. Although at a macroscopic scale, liquid illumination is performed by a light sheet, volume illumination is commonly used in microfluidics.[79] The flow rate is obtained from the integral of the velocity profile. Therefore, the height of the channel must be cut into multiple 2D planes. This method was first introduced in 1998 by Santiago *et al.* for microfluidics, and is referred to as micro-PIV.[80] These authors used epi-fluorescent illumination to record discrete particle images of fluorescent particles. They obtained the fluid velocity field with spatial resolutions of less than 10 μm. Meinhart *et al.* followed up this work using a similar technique with submicron resolution.[81] This can be achieved by epi-fluorescence microscopy coupled with high numerical aperture objectives, but better resolutions were obtained with confocal microscopy.[82] Other methods have been investigated such as defocused image analysis[83]

and digital holography.[84] However, they also require to scan the channel height, which remains a main drawback in flow rate measurement.

On the other hand, laser Doppler velocimetry relies on an interference fringe system with nearly parallel spacing d, which is formed by two intersecting coherent laser beams. When the particles seeded in the flow pass through the interference fringe system, they are alternately light and dark. The scattered light signal shows amplitude modulation with a Doppler frequency $f_{\text{Doppler}} = U/d$ corresponding to the particle velocity U orthogonal to the fringe spacing. However, as shown with the μ-PIV, scanning the channel height is required to measure the full velocity profile to obtain the flow rate.[85,86] A great improvement was made by Czarske *et al.* with the laser Doppler velocity profile sensor, which does not require the scanning of the channel height.[87] The position as well as the velocity of individual tracer particles are determined due to two superposed fan-like fringe systems, one being converging and the other one being diverging along the optical axis.

Although many advances have been made whether in μ-PIV to increase the scanning speed, or in laser Doppler with the addition of the laser Doppler flow profile sensor, these techniques were not turned into commercial end-user products due to two main limitations: its compacity and the particles themselves. The optical devices necessary to carry out measurements with seeded particles are far too voluminous (microscope, fast camera, objective, data processing) to be integrated in a fluidic circuit and are additionally expensive. However, this technique seems particularly suitable for sensor calibration. Thus, a holographic PIV system has been recently implemented at NIST to develop primary standards.[63] An original method has also been proposed using a rotating wheel asymmetrically positioned in a microfluidic channel.[88–90] The rotation arises from the dissipation of the liquid viscous stress at the surface of the wheel so that the flow measurement does not theoretically depend on the liquid viscosity. Thus, the rotation rate is linear to the flow rate. Even if such a sensor seems to be a promising solution as a disposable sensor, it gathers most of the limitations previously listed.

Flow sensors in microfluidics rely on a wide range of measurement principles. The technologies presented above have all been developed in academic laboratories, but their degree of maturity significantly varies and most of them have not yet led to routine end-user products. In this respect, two technologies stand out: thermal and Coriolis flowmeters. Commercial flowmeters dedicated to microfluidic applications and based on these two technologies are already on the market. However, the increasing part of life science applications in microfluidics has led to new needs, particularly for disposable sensors capable of measuring flow rates over wide ranges without prior calibration steps. This justifies further efforts to develop products based on principles not exploited yet commercially. Also, the diversification of microfluidic applications has increased the variety of needs regarding flow measurements. Among others, the nature of the liquids used and the range of flow rates varies significantly depending on the research field. This progressive complexification of the field, combined with the maturation of microfluidics into widely spread tools in industrial research, production, and diagnosis, call for increased normalization and standardization, and raise the need for methods and tools, allowing reliable comparison of these different technologies and traceability to primary existing standards. This is the role of metrology. Recent efforts have been made to adapt this field to low and very low flow rates to compare the performance of different flowmeters and provide standards and calibrations necessary for regulatory processes.

3 Metrology and primary standards for microfluidic flows

Until the 17th century, no global agreement or entities existed to define measurement ref. 91. The definition of units was extremely diverse regarding geographic dispersion. This was an obvious hurdle in equitable and efficient transactions. With the creation of the decimal unit system in 1799 and the development of experimental sciences, it appeared necessary to establish an independent international organization to coordinate the worldwide measurement system. The Meter Convention was ratified in Paris on May the 20th of 1875 by representatives of seventeen nations.[92] It settled the creation of the International Bureau of Weights and Measures (BIPM), an intergovernmental organization under the authority of the General Conference on Weights and Measures (CGPM), and the supervision of the International Committee for Weights and Measures (CIPM) to handle the demand for measurement standards. The National Metrology Institutes (NMIs) constitute the local relays of the international institutions. The global organization is completed by Regional Metrology Organizations (RMOs). Their main responsibilities are to facilitate traceability to primary standards, coordinate comparisons of national measurement standards, and update and share their facilities and knowledge. Over the years, the metrology system has evolved and other international organizations have been created to meet the needs of different aspects of metrology such as the International Organization of Standardization (ISO) and International Organization of Legal Metrology (OIML). Together, they closely cooperate and form the global metrology system. We review below the current achievements and progresses within the field of metrology for microfluidic flow measurements.

3.1 Development of primary standards for microfluidic flows

The development of primary standards relies on an international project organized within or between the RMOs by the NMIs. This development must follow a well-defined procedure to allow traceability of the measurements. Each

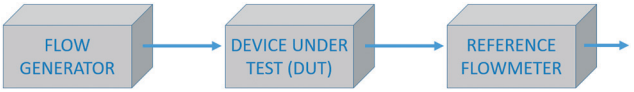

Fig. 6 Principle of primary standards for microflows.

NMI first develops its own flow sensor calibration system composed of a flow generator, a device under test (DUT), and a reference flowmeter, as shown in Fig. 6. To achieve a proper validation of the facilities, calibration systems must vary among NMIs to avoid systematic bias.[66] Once the system is implemented, a characterization is performed. Then each NMI claims its specifications and declares the nature of the liquids used, the flow rate measurements achieved, and their combined standard uncertainty (see the GUM for more information on uncertainty[93]). To validate the measurements and uncertainties claimed by each NMI for the whole flow range, results are submitted for intercomparisons. These intercomparisons are performed through at least two DUTs called transfer standards. The use of many transfer standards is required to prevent any systematic errors. It can either be a flowmeter or a flow actuator. The project pilot must calibrate the DUTs at the beginning and at the end of the intercomparisons. Each NMI is required to estimate the uncertainty due to drift. The measurements and their combined uncertainties obtained from the intercomparisons are then statistically analyzed and characterized by a consistency value (a detailed procedure of this statistical analysis can be found in ref. 94). These intercomparisons allow to support mutual confidence in calibration and measurement capabilities (CMCs).[95] The claimed CMCs, containing the flow range, uncertainties, and liquids used, are submitted to the belonging RMOs for validation. If validated, CMCs are then published in the BIPM key comparison database (KCDB).[96] Such projects allow the implementation of new calibration capacities. Academic labs, international flowmeter manufacturers, or other NMIs can thus use these facilities to validate and get accreditation for the performance of their technology or calibration services.

3.2 The metrology for drug delivery (MEDD) project

The development of primary standards for microfluidic flows was deemed necessary for scientific, economic, and public health reasons. Metrology institutes have seen a growing demand from flowmeter manufacturers to certify their technologies. Furthermore, the lack of facilities able to measure these flows has had a detrimental impact on clinical applications, in which its consequences can be particularly dramatic. Indeed, dosing errors in drug delivery have been shown to be one of the main causes of adverse patient incidents.[97–101] Precisely, numerous accidents (especially in neonatal care[100–102]) have been listed in the past years related to dosing errors in drug delivery by infusion.

In order to meet these needs, the European Metrology for Drug Delivery project (EMDD),[103] funded by the Euramet European Metrology Research Programme (EMRP), was started in 2012. So far, some metrological infrastructures have been developed for flow rates between 1.6 mL min^{-1} and 8.3 μL min^{-1} but neither characterized nor validated. To remedy this obvious lack of infrastructure capable of measuring microfluidic flows, the objectives of the MEDD project were to develop and characterize primary standards for liquid flow at atmospheric conditions for flow rates from 10 mL min^{-1} down to 1 nL min^{-1} with a target uncertainty better than 0.5% in steady state flows, to test commercially available flowmeters in various operation conditions, and finally to test drug delivery systems.

This project involves National Metrology Institutions (CETIAT (FR), DTI (DK), IPQ (P), METAS (SZ), VSL (NL), and MIKES VTT (FIN)), as well as industrial and academic partners (Bronkhorst High-Tech (NL) and FH Lubeck University (DE)).[65,66,94,98,104–109] Toward primary standards for microfluidic flows two methods have been investigated– the gravimetric principle and the front tracking meniscus in a capillary; only the first one was submitted for intercomparisons.†

3.3 Gravimetric flow rate measurement

The principle of gravimetric calibration systems is based on the measurement of the fluid mass over time. Knowing the liquid density ρ_l, the measurement of the mass increment Δm per unit time Δt allows the flow rate measurement.

$$Q = \frac{1}{\rho_l} \cdot \frac{\Delta m}{\Delta t} \tag{7}$$

The development of a primary standard allowing the traceability of microfluidic flow rate measurements can only be achieved with a high level of control of the flow stability, the quantities that define the liquid, and the mass measurement system. Liquid monitoring was performed either by a pressure controller or by syringe pumps. Flow stability is the most important parameter to control. The precision of the pressure control is based on a constant hydrodynamic resistance R_h of the fluidic system. R_h can be altered during the calibration by deformable tubing or by

† We also included recent development of primary standards at NIST based on the recent work of Schmidt *et al.*, though intercomparisons were made but not validated yet.[68] Moreover, we know some recent advances in calibration facilities could have been made in the different NMIs[63,67,116] but few characterizations were available and they weren't validated by means of intercomparisons. Consequently, changes in the calibration setup will just be mentioned. In addition, although CMCs claims concerned steady state flows calibration, facilities to measure pulsating flows were also investigated at METAS and DTI[117] but they won't be discuss in the scope of this review.

impurities in the liquid. Thus, in most cases, stainless steel tubings were used. Syringe pump actuation can be problematic when studying very low flow rates. Indeed, the fluctuations of the order of 10% have been observed in the flow rate ranges of the order of nL min^{-1}.[110] Water was used as the test liquid for the calibration of all systems. Special attention was paid to the water treatment. In most cases, ultrapure and degassed water was used as dust and bubbles can modify the resistance of the channel or even add a bias in the mass increment. The density of the liquid is taken to be a constant $\rho_l = 10^3$ kg m^{-3}. However, the lack of temperature control during the experiments can alter this parameter and thus increase the measurement error. The measurement precision is given by the resolution of the scale and its acquisition frequency. The measurements are obtained on a sampling period that allows to adapt to the mass increment, and to smooth the experimental noise by an average. However, the very low acquisition frequency of the scales used can be observed. Coupled with time averaging, these measurement systems represent a major limitation to observe flow rate fluctuations. With the aim of developing primary standards for dynamic flows, this technique seems inappropriate.

Two major sources of error emerged during flow rate calibration: the liquid evaporation and the interaction between the outlet of the fluidic system and the liquid in the beaker. These phenomena become much more significant as the studied flow rate decreases. To limit liquid evaporation that takes place in ambient air (a few μL min^{-1}), better results were achieved by covering the liquid with an oil layer (down to a tenth of a nL min^{-1}) than with air saturation in humidity (order of one μL min^{-1}). Second, the outlet needle is immersed in the liquid to prevent the flow from being dripped, causing a discontinuous measurement of the added mass. However, new sources of uncertainty arise from the interaction between the needle and the liquid. Firstly, the immersion of the needle in the liquid causes an addition of mass due to buoyancy. Indeed, the buoyancy increases as the beaker fills up. Increasing the surface area of the beaker would reduce this effect but would also result in greater evaporation. Secondly, the contact between the needle and the liquid results in capillary forces that should be taken into account with pressure actuation. The characterization of the error becomes significantly more difficult when using an oil layer to prevent evaporation. Attempts were made to calibrate these effects and account for them in the flow measurement. However, these results are preliminary and are subject to caution. Indeed, evaporation, buoyancy, and surface tension forces are correlated. The calculation of uncertainties becomes significantly more complex according to the GUM.[93] In addition, no mention was made of the hysteresis effect of the contact angle between the liquid and the needle, although this effect has been widely described in the microfluidic literature.[111,112] In order to take into account these sources of error in the flow measurement, eqn (7) was corrected. Depending on the setup and calibrations carried out, each NMI used its own working equation for flow. For instance, at NIST, eqn (7) becomes

$$Q = \frac{1}{\rho_l} \cdot \left[\frac{\Delta m_m \cdot f_b - \Delta m_{zero} + \Delta m_{evap}}{\Delta t} \cdot f_\gamma \right] \quad (8)$$

where ρ_l is the density of the flowing liquid, Δm is the mass difference read on the scale over Δt, and Δm_{zero} and Δm_{evap} respectively correspond to drift in mass and evaporation rates. Eventually, f_b and f_γ are the respective correction factors for buoyancy and surface tension. By taking the corrections into account in the measurement equation, the measurement precision increases. Due to the described measurement protocols, and taking into account the various sources of error, the different institutes could claim the performances of their calibration systems. As each NMI has developed its own procedure, significant differences were observed in both flow rate ranges and uncertainties claimed. Only three institutes (METAS, IPQ, DTI) have claimed that they are able to measure flow rates below the μL min^{-1} range but remain far from the objective of 1 nL min^{-1}. As described previously, intercomparisons were performed using transfer standards to validate these claims. In the MeDD project, a syringe pump (Nexus Syringe pump 300) and a Coriolis flowmeter (Bronkhorst Hi-Tech) were used as transfer standards at ambient conditions from 2 μL min^{-1} to 3 mL min^{-1}. The consistency of the measurements claimed by each of the institutes has been validated by means of intercomparisons, apart from the 3 mL min^{-1} value obtained at CETIAT. A detailed explanation of these intercomparisons can be found in ref. 94. Thus, the calibration facilities are operational and the various NMIs will submit their CMCs to EURAMET. If applicable, the NMIs will also get the accreditation according to ISO17025:2005 for the declared CMCs. So far, no CMC claims could be found in the KCDB. The conclusions of the project call into question the possibility to measure the flows of the order of the nL min^{-1} range. Moreover, these infrastructures have been developed using ultrapure water. A change in the liquid would require a similar development to calibrate the sources of error observed. Finally, this system is not suitable to test flowmeters with fluids whose vapor pressure is lower than water (typically fluorinated oil used in droplet microfluidics). Therefore, other possibilities have been investigated in particular using the front tracking meniscus method at Lubeck University and micro-PIV at NIST.[68]

3.4 Front tracking meniscus (FTM)

In response to the limitations of the gravimetric principle previously mentioned, investigations on the front tracking meniscus method were carried on by Lubeck University.[110,113] First investigated for low flow rate by Richter *et al.*,[114] this

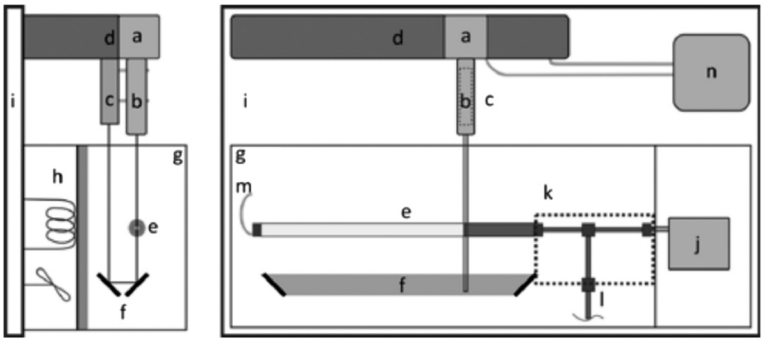

Fig. 7 Representation of the experimental setup for front tracking meniscus method. On the right: Top view. a) CCD camera, b) lens, c) LED, d) linear stage, e) capillary, f) mirrors, g) regulated chamber, h) heating element, i) vibration-free table, j) DUT, k) thermally-insulated fittings and tubing, l) valve, m) polymer tubing, n) PC. On the left: Side view.[113]

method relies on tracking the meniscus displacement of a flowing liquid in a capillary of known dimensions set at the outlet of the calibration system, as described in Fig. 7. The flow rate is measured according to

$$Q = \frac{\Delta x}{\Delta t} \cdot \Pi R^2 \tag{9}$$

where Δx is the meniscus displacement within the time interval Δt in a capillary with radius R. Using FTM allows to study flow rates much lower than the gravimetric system. As an example, using a capillary with an inner diameter of 150 μm and an optical system with a position uncertainty of 2 μm, 0.03 nL could be detected with the front tracking principle as compared to 1 nL ≈ 1 μg using a gravimetric setup.

Experiments were carried out with distilled, demineralized, and degassed water. The calibration system was used to evaluate a precision syringe pump and a commercial thermal flow sensor from 5 nL min^{-1} to 100 nL min^{-1}. To fully characterize the calibration system, numerous sources of uncertainty have been characterized on different variables such as Δt, Δx, and R through the law of propagation of uncertainties. For smaller flow rates or shorter sampling periods, the precision of the image process is the largest source of uncertainty. These effects are all the more important as the radius of the capillary increases. Moreover, as the curvature of the interface increases, the measurement of the meniscus position is affected. Conversely, when increasing the flow rate or for long sampling periods, the radius uncertainty is predominant.

Contrary to the gravimetric principle that could only measure flows in the μL min^{-1} range, FTM is able to probe flows down to nL min^{-1}; consequently, it is a calibration system much more adapted to microfluidic flow. Thus, CETIAT has recently started to develop a primary standard based on the FTM principle to decrease the minimum measurable flow.[115] However, it remains a metrological tool and cannot be used in an industrial or academic setting as a sensor. Indeed, the portability of the system does not meet the dimensioning of a microfluidic experiment, but above all, it can only be set at the outlet of the microfluidic circuit. This greatly restricts the fields of application of such a sensor.

4 Perspectives

Herein, we have reviewed the current strategies for microfluidic flow measurement, from their physical principles to their metrological aspects. We distinguished two main families, namely, active systems, in which energy is provided to the fluid and the measure is associated with the coupling of the flow with this energy transfer, and passive systems, measuring directly or indirectly the effect of the flow on a sensor. Currently, active systems cover the essentials of commercial products, the most widely used being the thermal sensors. Coriolis-based sensors have been proposed more recently and have gained interest in spite of their higher complexity and cost. This can be explained by their higher accuracy at very low flow and more "universal" character, notably due to their relative independence to the thermal and mechanical properties of the fluid. However, these commercial flowmeters are probably too expensive for many microfluidic applications; thus, we believe that the future needs will call for a renewal of interest in passive flow sensors and stimulate the maturation of at least some of the concepts recalled above (or new ones yet to be invented) into commercial products. Sensors based on pressure-differences may, in particular, be good candidates for not very demanding applications. They have the disadvantage of being dependant on the fluid's viscosity, but for numerous point-of-use or disposable applications, the gain in cost and simplicity may be worth the loss in the accuracy. This could be the case, for *e.g.*, for water monitoring (in which the fluid's viscosity does not vary much), cell culture, or organs-on-chip (in which only the orders of magnitude of flow rates may be sufficient, for *e.g.*, to ensure sufficient perfusion of nutriments or reagents).

On the application side, microfluidics expand toward more and more diverse research fields and markets, and we anticipate that this expansion will require further developments in flow measurement strategies. First, the development of instruments, notably for clinical use, requires very accurate and reliable

measurements and standardization. This is addressed by metrology, but there is still a delay and a performance gap between the development of flowmeters by academic and industrial players, and the development of primary standards within metrological institutes. Indeed, the first began in the 1970s and can reach tens of nL min^{-1}, while the second, developed since the 2010s, can only measure flow rates down to 2 μL min^{-1}. This partially explains the standardization problems encountered by microfluidics. As an obvious reason, metrology has the highest standards in terms of reliability and naturally tends to be more conservative (a trend to be paralleled with the also long delay between the discovery of new analytical technologies and their acceptance by health regulation authorities). Furthermore, establishing and maintaining comparability of measurement results can only be achieved through an international system that allows traceability from the measurement standard level (NMIs) down to routine field measurements. This is a multi-stakeholders process, which may also induce delays. To bridge the performance gap stated above, we suggest that a good compromise could be to accept that the idea that the sensors used for calibration are not "ultimate" versions of the commercial ones they check but based on different principles limited to calibration purposes (*e.g.*, front meniscus or gravimetric measurements), and restrict calibration to long steady-state measurements. This would have the disadvantage of not ensuring the full certification of the stability of the sensors but could still constitute a first useful step for the certification of low flow rate sensors.

Conflicts of interest

Jean-Louis Viovy is a cofounder/shareholder of Fluigent.

References

1 D. Qin, Y. Xia, J. A. Rogers, R. J. Jackman, X.-M. Zhao and G. M. Whitesides, *Microfabrication, Microstructures and Microsystems*, 1998, pp. 1–20.
2 G. M. Whitesides, The origins and the future of microfluidics, *Nature*, 2006, **442**(7101), 368–373.
3 N. Convery and N. Gadegaard, 30 Years of Microfluidics, *Micro Nano Eng.*, 2019, **2**, 76–91.
4 H. A. Stone, A. D. Stroock and A. Ajdari, Engineering Flows in Small Devices, *Annu. Rev. Fluid Mech.*, 2004, **36**(1), 381–411.
5 R. G. Sweet, High frequency recording with electrostatically deflected ink jets, *Rev. Sci. Instrum.*, 1965, **36**(2), 131–136.
6 F. C. M. van de Pol and J. Branebjerg, Micro fluid-handling systems: state of the art and opportunities, in *Fifth International Conference on Advanced Robotics'Robots in Unstructured Environments*, IEEE, 1991, vol. 1, pp. 283–290, Available from: **https://ieeexplore.ieee.org/document/240639/**.
7 E. Bassous, H. H. Taub and L. Kuhn, Ink jet printing nozzle arrays etched in silicon, *Appl. Phys. Lett.*, 1977, **31**(2), 135–137.
8 S. C. Terry, *A gas chromatography system fabricated on a silicon wafer using integrated circuit technology*, Stanford University, 1975.
9 S. C. Terry, J. H. Herman and J. B. Angell, A Gas Chromatographic Air Analyzer Fabricated on a Silicon Wafer, *IEEE Trans. Electron Devices*, 1979, **26**(12), 1880–1886.
10 A. Manz, N. Graber and H. M. Widmer, Miniaturized total chemical analysis systems: A novel concept for chemical sensing, *Sens. Actuators, B*, 1990, **1**(1–6), 244–248.
11 C. M. Hindson, J. R. Chevillet, H. A. Briggs, E. N. Gallichotte, I. K. Ruf and B. J. Hindson, *et al.* Absolute quantification by droplet digital PCR versus analog real-time PCR, *Nat. Methods*, 2013, **10**(10), 1003–1005, Available from: **https://www.nature.com/articles/nmeth.2633**.
12 A. A. Morley, Digital PCR: A brief history, *Biomol. Detect. Quantif.*, 2014, **1**(1), 1–2, Available from: **https://linkinghub.elsevier.com/retrieve/pii/S2214753514000023**.
13 M. Verhulsel, M. Vignes, S. Descroix, L. Malaquin, D. M. Vignjevic and J.-L. Viovy, A review of microfabrication and hydrogel engineering for micro-organs on chips, *Biomaterials*, 2014, **35**(6), 1816–1832, Available from: **https://linkinghub.elsevier.com/retrieve/pii/S0142961213013744**.
14 L. A. Low, C. Mummery, B. R. Berridge, C. P. Austin and D. A. Tagle, Organs-on-chips: into the next decade, *Nat. Rev. Drug Discovery*, 2021, **20**(5), 345–361, **https://www.nature.com/articles/s41573-020-0079-3**.
15 D. E. Ingber, Human organs-on-chips for disease modelling, drug development and personalized medicine, *Nat. Rev. Genet.*, 2022, DOI: **10.1038/s41576-022-00466-9**.
16 Markets and Markets (2013) Microfluidics market by materials (polymers, silicon, glass), pharmaceuticals (microreactors, toxicity screening, lab on chip, proteomic & genomic analysis) drug delivery devices(microneedles, micropumps), IVD (POC)–global tr.
17 Microfluidics Market by Product (Devices, Components (Chips, Sensors, Pump, Valves, and Needles)), Application (IVD [POC, Clinical, Veterinary], Research, Manufacturing, Therapeutics), End User and Region – Global Forecast to 2025.
18 C. D. Chin, V. Linder and S. K. Sia, Commercialization of microfluidic point-of-care diagnostic devices, *Lab Chip*, 2012, **12**(12), 2118–2134.
19 P. S. Dittrich and A. Manz, Lab-on-a-chip: Microfluidics in drug discovery, *Nat. Rev. Drug Discovery*, 2006, **5**(3), 210–218.
20 S. Yadav, *Analysis of value creation and value capture in microfluidics market*, Massachusetts Institute of Technology, Engineering Systems Division, 2010, Available from: **https://dspace.mit.edu/handle/1721.1/59276**.
21 *Micro System Technologies 90*, Micro Liquid-Handling Devices – A Review, in Intergovernmental Panel on Climate Change, ed. F. C. M. Van De Pol and J. Branebjerg, Springer Berlin, Heidelberg, Berlin, Heidelberg, 1990, pp. 799–805, Available from: **https://www.cambridge.org/core/product/identifier/CBO9781107415324A009/type/book_part**.

22 P. Gravesen, J. Branebjerg and O. S. Jensen, Microfluidics - A review, *J. Micromech. Microeng.*, 1993, **3**(4), 168–182, Available from: **https://iopscience.iop.org/0960-1317/3/4/002**.

23 H. Van Heeren, *Results survey on microfluidics & sensors*, 2016, July.

24 International vocabulary of metrology–Basic and general concepts and associated terms, in *International vocabulary of metrology(VIM)*, 2012, **https://www.nist.gov/system/files/documents/pml/div688/grp40/International-Vocabulary-of-Metrology.pdf**.

25 N. Nguyen, Micromachined flow sensors—a review, *Flow Meas. Instrum.*, 1997, **8**(1), 7–16, Available from: **https://linkinghub.elsevier.com/retrieve/pii/S0955598697000198**.

26 J. T. W. Kuo, L. Yu and E. Meng, Micromachined thermal flow sensors-A review, *Micromachines*, 2012, **3**(3), 550–573.

27 F. Ejeian, S. Azadi, A. Razmjou, Y. Orooji, A. Kottapalli and M. Ebrahimi Warkiani, *et al.*, Design and applications of MEMS flow sensors: A review. Sensors Actuators, *Sens. Actuators, A*, 2019, **295**, 483–502, DOI: **10.1016/j.sna.2019.06.020**.

28 C. Liu, Micromachined biomimetic artificial haircell sensors, *Bioinspiration Biomimetics*, 2007, **2**(4), S162–S169.

29 F. Rizzi, A. Qualtieri, T. Dattoma, G. Epifani and M. De Vittorio, Biomimetics of underwater hair cell sensing, *Microelectron. Eng.*, 2015, **132**, 90–97.

30 S. Silvestri and E. Schena, Micromachined flow sensors in biomedical applications, *Micromachines*, 2012, **3**(2), 225–243.

31 A. F. P. Van Putten and S. Middelhoek, Integrated silicon anemometer, *Electron. Lett.*, 1974, **10**(21), 425–426.

32 T. E. Miller and H. Small, Thermal Pulse Time-of-Flight Liquid Flow Meter, *Anal. Chem.*, 1982, **54**(6), 907–910.

33 H. Heeren, *Results survey on microfluidics flow control*, 2016.

34 L. V. King, XII. On the convection of heat from small cylinders in a stream of fluid: Determination of the convection constants of small platinum wires with applications to hot-wire anemometry, *Philos. Trans. R. Soc., A*, 1914, **214**(509–522), 373–432, DOI: **10.1098/rsta.1914.0023**.

35 S. Wu, Q. Lin, Y. Yuen and Y. C. Tai, MEMS flow sensors for nano-fluidic applications, *Sens. Actuators, A*, 2001, **89**(1–2), 152–158.

36 E. Meng and Y. C. Tai, A parylene MEMS flow sensing array, *Transducers 2003 – 12th Int Conf Solid-State Sensors, Actuators Microsystems, Dig Tech Pap.*, 2003, vol. 1, pp. 686–689.

37 B. Mimoun, A. van der Horst, R. Dekker, D. van der Voort, A. van der Horst and M. Rutten, *et al.*, Thermal flow sensors on flexible substrates for minimally invasive medical instruments, in *2012 IEEE Sensors*, IEEE, 2012, pp. 1–4, Available from: **https://ieeexplore.ieee.org/document/6411429/**.

38 T. S. J. Lammerink, N. R. Tas, M. Elwenspoek and J. H. J. Fluitman, Micro-liquid flow sensor, *Sens. Actuators, A*, 1993, **37–38**, 45–50, Available from: **https://linkinghub.elsevier.com/retrieve/pii/092442479380010E**.

39 P. Fürjes, G. Légrádi, C. Dücső, A. Aszódi and I. Bársony, Thermal characterisation of a direction dependent flow sensor, *Sens. Actuators, A*, 2004, **115**(2–3), 417–423, Available from: **https://linkinghub.elsevier.com/retrieve/pii/S0924424704003401**.

40 M. Dijkstra, M. J. de Boer, J. W. Berenschot, T. S. J. Lammerink, R. J. Wiegerink and M. Elwenspoek, Miniaturized flow sensor with planar integrated sensor structures on semicircular surface channels, in *2007 IEEE 20th International Conference on Micro Electro Mechanical Systems(MEMS)*, IEEE, 2007, pp. 123–126, Available from: **https://ieeexplore.ieee.org/document/4433031/**.

41 N. T. Nguyen, X. Y. Huang and K. C. Toh, Thermal flow sensor for ultra-low velocities based on printed circuit board technology, *Meas. Sci. Technol.*, 2001, **12**(12), 2131–2136.

42 R. Antony, M. S. Giri Nandagopal, N. Sreekumar and N. Selvaraju, Detection principles and development of microfluidic sensors in the last decade, *Microsyst. Technol.*, 2014, **20**(6), 1051–1061, DOI: **10.1007/s00542-014-2165-0**.

43 H. Berthet, J. Jundt, J. Durivault, B. Mercier and D. Angelescu, Time-of-flight thermal flowrate sensor for lab-on-chip applications, *Lab Chip*, 2011, **11**(2), 215–223.

44 **https://www.fluigent.com/product/microfluidic-components/frp-flow-rate-platform/**.

45 S. Deng, P. Wang, S. Liu, T. Zhao, S. Xu and M. Guo, *et al.*, A Novel Microfluidic Flow Rate Detection Method Based on Surface Plasmon Resonance Temperature Imaging, *Sensors*, 2016, **16**(7), 964, Available from: **https://www.mdpi.com/1424-8220/16/7/964**.

46 Y. Kikutani, K. Mawatari, K. Katayama, M. Tokeshi, T. Fukuzawa and M. Kitaoka, *et al.*, Flowing thermal lens micro-flow velocimeter, *Sens. Actuators, B*, 2008, **133**(1), 91–96.

47 G. G. Coriolis, Mémoire sur les équations du mouvement relatifs des systèmes de corps, *Journal de l'École polytechnique*, 1835, 142–154.

48 P. Enoksson, G. Stemme and E. Stemme, A silicon resonant sensor structure for coriolis mass-flow measurements, *J. Microelectromech. Syst.*, 1997, **6**(2), 119–125.

49 **https://www.bronkhorst.com/int/products/liquid-flow/mini-cori-flow/**.

50 J. Groenesteijn, Microfluidic platform for Coriolis-based sensor and actuator systems, *PhD*, University of Twente, 2016, DOI: **10.3990/1.9789036540117**.

51 J. Haneveld, T. S. J. Lammerink, M. J. De Boer, R. G. P. Sanders, A. Mehendale and J. C. Lötters, Modeling, design, fabrication and characterization of a micro Coriolis mass flow sensor, *J. Micromech. Microeng.*, 2010, **20**(12), 125001.

52 T. V. P. Schut, D. Alveringh, W. Sparreboom, J. Groenesteijn, R. J. Wiegerink and J. C. Lotters, Fully integrated mass flow, pressure, density and viscosity sensor for both liquids and gases, in *2018 IEEE Micro Electro Mechanical Systems(MEMS)*. IEEE, 2018, pp. 218–221, Available from: **https://ieeexplore.ieee.org/document/8346523/**.

53 M. A. Boillat, A. J. van der Wiel, A. C. Hoorgerwerf and N. F. de Rooij, Differential pressure liquid flow sensor for flow regulation and dosing systems, *Proc. - IEEE Micro Electro Mech. Syst., 8th*, 1995, 350–352.
54 T. Rodrigues, F. J. Galindo-Rosales and L. Campo-Deaño, Towards an optimal pressure tap design for fluid-flow characterisation at microscales, *Materials*, 2019, **12**(7), 8–10.
55 R. E. Oosterbroek, T. S. J. Lammerink, J. W. Berenschot, G. J. M. Krijnen, M. C. Elwenspoek and A. van den Berg, A micromachined pressure/flow-sensor, *Sens. Actuators, A*, 1999, **77**(3), 167–177, Available from: **https://linkinghub.elsevier.com/retrieve/pii/S0924424799001880**.
56 A. Shakir, K. Srihari, B. Murcko, C. Yun and B. Sulouff, Flow sensor using micromachined pressure sensor, *Proc IEEE Sensors*, 2008, pp. 62–65.
57 *SLG Liquid Flow Meter Series*, 2020, Available from: **https://sensirion.com/media/documents/69EBDF62/61658A36/Sensirion_Liquid_Flow_Meters_SLG_Datasheet_1.pdf**.
58 *SLI Liquid Flow Meter Series*, 2020, Available from: **https://sensirion.com/media/documents/9D0BBC1B/616588DA/Sensirion_Liquid_Flow_Meters_SLI_Datasheet.pdf**.
59 R. Ahrens and K. Schlote-Holubek, A micro flow sensor from a polymer for gases and liquids, *J. Micromech. Microeng.*, 2009, **19**(7), 074006.
60 *mini Cori-Flow Series ML120*, Available from: **https://www.bronkhorst.com/getmedia/9dc94505-0494-43fc-ac6a-de18019932ce/mini-cori-flow-ml120.pdf**.
61 N. Noeth, S. S. Keller and A. Boisen, Integrated cantilever-based flow sensors with tunable sensitivity for in-line monitoring of flow fluctuations in microfluidic systems, *Sensors*, 2013, **14**(1), 229–244.
62 V. Gass, B. H. van der Schoot and N. F. de Rooij, Nanofluid handling by micro-flow-sensor based on drag force measurements, *Proc. - IEEE Micro Electro Mech. Syst., 8th*, 1993, 167–172.
63 P. Salipante, S. D. Hudson, J. W. Schmidt and J. D. Wright, Microparticle tracking velocimetry as a tool for microfluidic flow measurements, *Exp. Fluids*, 2017, **58**(7), 1–10.
64 M. Ahrens, S. Klein, B. Nestler and C. Damiani, Design and uncertainty assessment of a setup for calibration of microfluidic devices down to 5 nL min-1, *Meas. Sci. Technol.*, 2014, **25**(1), 015301.
65 H. Bissig, H. T. Petter, P. Lucas, E. Batista, E. Filipe and N. Almeida, *et al.*, Primary standards for measuring flow rates from 100 nl/min to 1 ml/min-gravimetric principle, *Biomed. Tech.*, 2015, **60**(4), 301–316.
66 *EURAMET, Final Publishable JRP Report MetroNORM: IND57*, Eur Metrol Res Program, 2017, (July), p. 28, Available from: **https://metronorm-emrp.eu/wp-content/uploads/2017/08/IND57-MetroNORM-Final-publishable-JRP-report-approved.pdf**.
67 O. Florestan, M. Sandy and S. Julien, Recent improvements of the French liquid micro-flow reference facility, *Meas. Sci. Technol.*, 2018, **29**(2), aa97ef, DOI: **10.1088/1361-6501/aa97ef**.
68 J. W. Schmidt and J. D. Wright, Micro-flow calibration facility at NIST, in *9th ISFFM*, 2015.
69 J. S. Wexler, P. H. Trinh, H. Berthet, N. Quennouz, O. Du Roure and H. E. Huppert, *et al.* Bending of elastic fibres in viscous flows: The influence of confinement, *J. Fluid Mech.*, 2013, **720**, 517–544.
70 B. Semin, J. P. Hullin and H. Auradou, Influence of flow confinement on the drag force on a static cylinder, *Phys. Fluids*, 2009, **21**(10), 1–9.
71 N. Noeth, S. S. Keller and A. Boisen, Fabrication of a cantilever-based microfluidic flow meter with nL min −1 resolution, *J. Micromech. Microeng.*, 2011, **21**(1), 015007.
72 R. Attia, D. C. Pregibon, P. S. Doyle, J. L. Viovy and D. Bartolo, Soft microflow sensors, *Lab Chip*, 2009, **9**(9), 1213–1218.
73 D. Dendukuri, D. C. Pregibon, J. Collins, T. A. Hatton and P. S. Doyle, Continuous-flow lithography for high-throughput microparticle synthesis, *Nat. Mater.*, 2006, **5**(5), 365–369.
74 D. Dendukuri, S. S. Gu, D. C. Pregibon, T. A. Hatton and P. S. Doyle, Stop-flow lithography in a microfluidic device, *Lab Chip*, 2007, **7**(7), 818–828.
75 J. Tao and X. Yu, Hair flow sensors: From bio-inspiration to bio-mimicking - A review, *Smart Mater. Struct.*, 2012, **21**(11), 113001.
76 L. Zhang, X. Yu, S. You, H. Liu, C. Zhang and B. Cai, Highly sensitive microfluidic flow sensor based on aligned piezoelectric poly(vinylidene fluoride-trifluoroethylene) nanofibers, *Appl. Phys. Lett.*, 2015, **107**(24), 242901.
77 J. M. Engel, J. Chen, C. Liu and D. Bullen, Polyurethane rubber all-polymer artificial hair cell sensor, *J. Microelectromech. Syst.*, 2006, **15**(4), 729–736.
78 N. Chen, C. Tucker, J. M. Engel, Y. Yang, S. Pandya and C. Liu, Design and Characterization of Artificial Haircell Sensor for Flow Sensing With Ultrahigh Velocity and Angular Sensitivity, *J. Microelectromech. Syst.*, 2007, **16**(5), 999–1014, DOI: **10.1109/JMEMS.2007.902436**.
79 S. T. Wereley and C. D. Meinhart, Recent Advances in Micro-Particle Image Velocimetry, *Annu. Rev. Fluid Mech.*, 2010, **42**(1), 557–576.
80 G. J. Santiago, T. S. Wereley, D. C. Meinhart, J. D. Beebe and J. R. Adrian, A particle image velocimetry system for microfluidics, *Exp. Fluids*, 1998, **25**(4), 316–319, DOI: **10.1007/s003480050235**.
81 C. D. Meinhart, S. Wereley and M. Gray, Volume illumination for two-dimensional particle image velocimetry, *Meas. Sci. Technol.*, 2000, **11**(6), 809–814.
82 J. S. Park, C. K. Choi and K. D. Kihm, Optically sliced micro-PIV using confocal laser scanning microscopy(CLSM), *Exp. Fluids*, 2004, **37**(1), 105–119.
83 J. S. Park and K. D. Kihm, Three-dimensional micro-PTV using deconvolution microscopy, *Exp. Fluids*, 2006, **40**(3), 491–499.
84 S. Kim and S. J. Lee, Measurement of 3D laminar flow inside a micro tube using micro digital holographic particle tracking velocimetry, *J. Micromech. Microeng.*, 2007, **17**(10), 2157–2162, DOI: **10.1088/0960-1317/17/10/030**.
85 L. Buettner and J. Czarske, A multimode-fibre laser-Doppler anemometer for highly spatially resolved velocity measurements using low-coherence light, *Meas. Sci. Technol.*, 2001, **12**(11), 1891–1903.

86 A. K. Tieu, M. R. Mackenzie and E. B. Li, Measurements in microscopic flow with a solid-state LDA, *Exp. Fluids*, 1995, **19**(4), 293–294.
87 J. Czarske, L. Büttner, T. Razik and H. Müller, Boundary layer velocity measurements by a laser Doppler profile sensor with micrometre spatial resolution, *Meas. Sci. Technol.*, 2002, **13**(12), 1979–1989.
88 B. U. Moon, S. S. H. Tsai and D. K. Hwang, Rotary polymer micromachines: in situ fabrication of microgear components in microchannels, *Microfluid. Nanofluid.*, 2015, **19**(1), 67–74.
89 R. Attia, *Modifications de surfaces et integration de MEMS pour les laboratoires sur puce*, 2010.
90 C. Cavaniol, *Towards a universal flow sensor for Microfluidics*, 2020.
91 J.-P. Fanton, A brief history of metrology: past, present, and future, *Int. J. Metrol. Qual. Eng.*, 2019, **10**(8), 5, DOI: **10.1051/ijmqe/2019005**.
92 CGPM, *La conférence du mètre*, Documents Diplomatiques, 1875.
93 Guide to the expression of uncertainty of measurement, in *ISO/IEC GUIDE 98-3:2008(E) Contents*, 2008, Available from: **https://isotc.iso.org/livelink/livelink/fetch/2000/2122/4230450/8389141/ISO_IEC_Guide_98-3_2008%28E%29_-_Uncertainty_of_measurement_-_Part_3%2C_Guide_to_the_expression_of_uncertainty_in_measurement_%28GUM%2C1995%29.pdf?nodeid=8389142&vernum=-2**.
94 P. Lucas, *Comparison of standards for low liquid flow rates*, 2017, EURAMET pr.
95 *Calibration and Measurement Capabilities(CMCs): A paper by the joint BIPM/ILAC WG(2007)*, 2007, pp. 1–6.
96 **https://www.bipm.org/kcdb/**.
97 A. F. Al-Assaf, L. J. Bumpus, D. Carter and S. B. Dixon, Preventing errors in healthcare: a call for action, *Hosp. Top.*, 2003, **81**(3), 5–13.
98 A. M. Timmerman, R. A. Snijder, P. Lucas, M. C. Lagerweij, J. H. Radermacher and M. K. Konings, How physical infusion system parameters cause clinically relevant dose deviations after setpoint changes, *Biomed. Tech.*, 2015, **60**(4), 365–376.
99 S. Klein and P. Lucas, Low liquid flows-an important aspect in medical technology, *Biomed. Tech.*, 2015, **60**(4), 269–270.
100 P. T. Lee, F. Thompson and H. Thimbleby, Analysis of infusion pump error logs and their significance for health care, *Br. J. Nurs.*, 2012, **21**(Sup 8), S12–S20, DOI: **10.12968/bjon.2012.21.Sup8.S12**.
101 R. A. Snijder, M. K. Konings, P. Lucas, T. C. Egberts and A. D. Timmerman, Flow variability and its physical causes in infusion technology: a systematic review of in vitro measurement and modeling studies, *Biomed. Tech.*, 2015, **60**(4), 277–300, Available from: **https://www.degruyter.com/view/j/bmte.2015.60.issue-4/bmt-2014-0148/bmt-2014-0148.xml**.
102 A. C. Van Der Eijk, R. M. F. P. T. Van Rens, J. Dankelman and B. J. Smit, A literature review on flow-rate variability in neonatal IV therapy, *Paediatr. Anaesth.*, 2013, **23**(1), 9–21.
103 **https://www.drugmetrology.com/**.
104 E. Batista, N. Almeida, A. Furtado, E. Filipe, L. Sousa and R. F. Martins, *et al.*, Assessment of drug delivery devices, *Biomed. Tech.*, 2015, **60**(4), 347–357.
105 F. Ogheard, A. K. Niemann, E. Batista, H. Bissig, A. M. Timmerman and R. A. Snijder, *et al.*, *Assessment of drug delivery devices and accessories A few show cases Flow rate error, compliance and impact of operating conditions*, 2015.
106 F. Ogheard, S. Margot and J. Savary, *Experimental study of buoyancy and surface tension effects of an immersed capillary gravimetric micro-flow facility*, 2016.
107 H. Bissig, M. Tschannen and M. de Huu, Micro-flow facility for traceability in steady and pulsating flow, *Flow Meas. Instrum.*, 2015, **44**, 34–42, DOI: **10.1016/j.flowmeasinst.2014.11.008**.
108 P. Lucas, M. Ahrens, J. Geršl, W. Sparreboom and J. Lötters, Primary standard for liquid flow rates between 30 and 1500 nl/min based on volume expansion, *Biomed. Tech.*, 2015, **60**(4), 317–335.
109 P. Lucas, *Primary standard nanoflow rates Overview of this presentation Low to ultra-low flow rates Presenting the results of MeDD Today' s program Part I and II*, 2014, (September 2013).
110 M. Ahrens, S. Klein, B. Nestler and C. Damiani, Design and uncertainty assessment of a setup for calibration of microfluidic devices down to 5 nL min-1, *Meas. Sci. Technol.*, 2014, **25**(1), 015301, Available from: **https://stacks.iop.org/0957-0233/25/i=1/a=015301?key=crossref.2ea028aba7915d5352938678fb9bd1b9**.
111 L. Leger and J. F. Joanny, Liquid spreading, *Rep. Prog. Phys.*, 1992, **55**(4), 431–486, Available from: **https://stacks.iop.org/0034-4885/55/i=4/a=001?key=crossref.e2191f33f9e732f5779fece847bdb224**.
112 J. F. Joanny and P. G. de Gennes, A new model for contact angle hysteresis, *J. Chem. Phys.*, 1984, **2**(2), 211–225.
113 M. Ahrens, B. Nestler, S. Klein, P. Lucas, H. T. Petter and C. Damiani, An experimental setup for traceable measurement and calibration of liquid flow rates down to 5 nl/min, *Biomed. Tech.*, 2015, **60**(4), 337–345.
114 M. Richter, P. Woias and D. Weiss, Microchannels for applications in liquid dosing and flow-rate measurement, *Sens. Actuators, A*, 1997, **62**(1–3 pt 3), 480–483.
115 F. Ogheard, P. Cassette and A. W. Boudaoud, Development of an optical measurement method for "sampled" micro-volumes and nano-flow rates, *Flow Meas. Instrum.*, 2020, **73**, 101746, DOI: **10.1016/j.flowmeasinst.2020.101746**.
116 H. Bissig, M. Tschannen and M. De Huu, Improving process quality by means of accurate and traceable calibration of flow devices with process-oriented liquids, *Chimia*, 2018, **72**(3), 124–129.
117 H. Bissig and A. K. Niemann, *Cross check of the pulsating flow tester at DTI and METAS*, 2014, pp. 1–37, **http://www.drugmetrology.com/wp-content/uploads/2016/09/2014_10_14_D_2_1_5_Report_Puls_Cross_Check_METAS.pdf**.
118 R. Monge, J. Groenesteijn, D. Alveringh, R. J. Wiegerink, J. Lötters and L. J. Fernandez, SU–8 micro coriolis mass flow sensor, *Sens. Actuators, B*, 2017, **241**, DOI: **10.1016/j.snb.2016.10.133**.